Martian Core Analysis

1. Module 1: Understanding Seismic Wave Velocities

1.1. What are P-waves and S-waves? Briefly describe their properties and how they differ in terms of the materials they can propagate through.

1.1.1. Introduction

Seismic waves are vibrations generated by earthquakes or other geophysical phenomena, propagating through Earth's interior. They are broadly categorized into Primary (P) and Secondary (S) waves. Understanding their characteristics is critical for seismic studies and geophysics.

1.1.2. P Waves (Primary Waves)

P waves are compressional waves capable of traveling through both solid and liquid media. These waves are the fastest seismic waves and are usually the first to be detected by seismometers after an earthquake.

- **Velocity**: P waves travel at speeds of 5–8 km/s in Earth's crust and faster in denser materials such as the mantle.
- **Path**: They follow a curved trajectory due to the varying density and composition of Earth's layers, because of which the velocity of P waves varies with distance from the Earth's core, refracting as they traverse different materials.
- **Shadow Zone**: P waves exhibit a shadow zone between 104° and 140° from the earthquake's focus due to refraction at the core-mantle boundary (Figure 1).

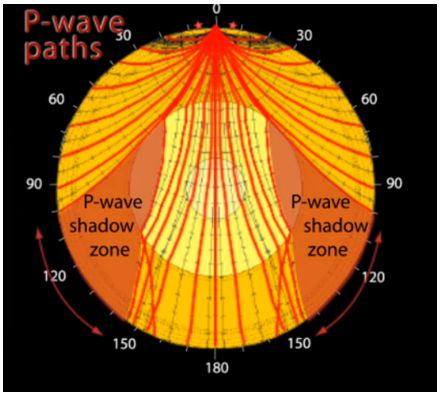

Figure 1: Path and shadow zone of P waves.

1.1.3. S Waves (Secondary Waves)

S waves are shear waves that only propagate through solids due to their transverse motion. These waves are slower than P waves, traveling at approximately 60% of the P wave velocity.

- **Velocity**: The speed of S waves is significantly affected by the rigidity of the material they pass through, ranging from 3–4 km/s in Earth's crust.
- **Path**: Like P waves, they are refracted by changes in material properties but are unable to penetrate the liquid outer core, creating a larger shadow zone (Figure 2).
- **Shadow Zone**: S waves generate a broad shadow zone beyond 104° due to their inability to traverse liquids.

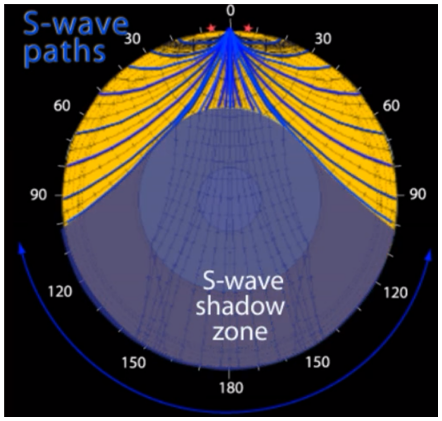

Figure 2: Path and shadow zone of S waves.

1.1.4. Conclusion

The study of P and S waves provides valuable insights into the Earth's internal structure. The distinct behaviors of these waves, particularly their interaction with different materials, have been instrumental in confirming the presence of Earth's liquid outer core and solid inner core.

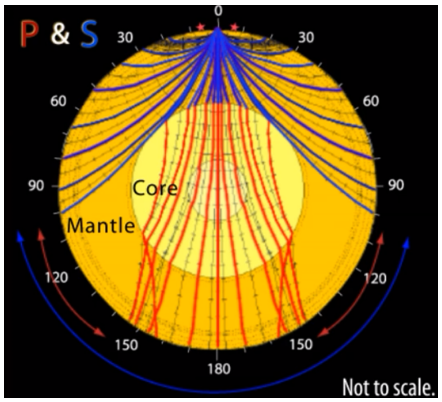

Figure 3: Comparison of P and S waves.

1.2. *Using the following equations for wave velocities, calculate the P-wave v_p and S-wave s_v velocities if the bulk modulus (K) is* 2.5×10^{10} *Pa, the shear modulus (G) is* 1.0×10^{10} *Pa, and the density (ρ) is 3000* kg/m^3

.

We know:

$$V_p = \sqrt{\frac{\lambda + 2\mu}{\rho}}$$

$$V_s = \sqrt{\frac{\mu}{\rho}}$$

$$\lambda = K - \frac{2}{3}g$$

K = bulk modulus
μ = shear modulus=g
ρ = density.

For V_p:

$$V_p = \sqrt{\frac{K + \frac{4}{3}g}{\rho}}$$

$$V_p = \sqrt{\frac{2.5 \times 10^{10} + \frac{4}{3} \cdot 10^{10}}{3 \times 10^3}}$$

$$= \sqrt{\frac{11.5 \times 10^7}{9}}$$

$$= \sqrt{\frac{115 \times 10^6}{9}}$$

$$= \sqrt{10723.8063}$$

$$= 3574.6018\,\text{m/s}$$

For V_s:

$$V_s = \sqrt{\frac{g}{\rho}}$$

$$V_s = \sqrt{\frac{10^{10}}{3 \times 10^3}}$$

$$= \sqrt{\frac{10^7}{3}}$$

$$= 1825.7419\,\text{m/s}$$

1.3. *Derive P and S waves in a homogeneous, isotropic medium.*

We already know that for an elastic wave traveling in a homogeneous isotopic medium,

$$\rho \partial_t^2 u_i = \partial_j \sigma_{ij} \tag{1}$$

(Note: We are using the Einstein summation convention here. The RHS is a sum over the repeated index j from 1 to 3.)

Here:

- ρ is the density.
- $\mathbf{u}$ is the displacement vector field. u_i is the ith component of the displacement vector field.
- λ and μ are Lamé parameters.
- σ_{ij} is the ijth component of the stress tensor.

Also according to Hooke's law,

$$\sigma_{ij} = \lambda\delta_{ij}(\nabla \cdot \mathbf{u}) + \mu\left(\frac{\partial u_i}{\partial x_j} + \frac{\partial u_j}{\partial x_i}\right)$$

$$\therefore \sigma_{ij} = \lambda\partial_k u_k \delta_{ij} + \mu\left(\partial_i u_j + \partial_j u_i\right) \quad (2)$$

Substituting (2) in (1),

$$\begin{aligned}\rho\partial_t^2 u_i &= \partial_j\left(\lambda\partial_k u_k\delta_{ij} + \mu(\partial_i u_j + \partial_j u_i)\right)\\ &= \lambda\partial_i\partial_k u_k + \mu\partial_j\partial_j u_i + \mu\partial_i\partial_j u_j\\ &= \lambda\partial_i\partial_j u_j + \mu\partial_j\partial_j u_i + \mu\partial_j\partial_i u_j\\ &= (\lambda+2\mu)\partial_i\partial_j u_j - \mu\left(\partial_i\partial_j u_j - \partial_j\partial_j u_i\right)\end{aligned}$$

$$\begin{aligned}\rho\partial_t^2 u_i\mathbf{e}_i &= (\lambda+2\mu)\partial_i(\nabla\cdot\mathbf{u})\mathbf{e}_i\\ &\quad - \mu\left(\partial_i(\nabla\cdot\mathbf{u})\mathbf{e}_i - \nabla^2 u_i\mathbf{e}_i\right)\end{aligned}$$

$$\rho\partial_t^2 u_i\mathbf{e}_i = (\lambda+2\mu)\nabla(\nabla\cdot\mathbf{u}) - \mu\left(\nabla(\nabla\cdot\mathbf{u}) - \nabla^2\mathbf{u}\right)$$

Now, using the identity:

$$\nabla(\nabla\cdot\mathbf{u}) - \nabla^2\mathbf{u} = \nabla\times(\nabla\times\mathbf{u})$$

We can write:

$$\rho\frac{\partial^2\mathbf{u}}{\partial t^2} = (\lambda+2\mu)\nabla(\nabla\cdot\mathbf{u}) - \mu\nabla\times(\nabla\times\mathbf{u}) \quad (3)$$

Rather than directly solving the wave equation derived on the previous slide, we can express the displacement field in terms of two other functions, a scalar $\Phi(x,t)$ and a vector $\Psi(x,t)$, via Helmholtz's theorem:

$$\mathbf{u} = \nabla\Phi + \nabla\times\Psi$$

In this representation, the displacement is the sum of the gradient of a scalar potential and the curl of a vector potential. Although this representation of the displacement field would at first appear to introduce complexity, it actually clarifies the problem because of the following two vector identities:

$$\nabla\times(\nabla\Phi) = 0$$
$$\nabla\cdot(\nabla\times\Psi) = 0$$

Due to the form of the RHS of the wave equation, these two vector identities separate the displacement field into two parts:

- $\nabla\Phi$: No curl or rotation, gives rise to compressional waves.
- $\nabla\times\Psi$: Zero divergence, causes no volume change, corresponds to shear waves.

If we now substitute $\mathbf{u} = \nabla\Phi + \nabla\times\Psi$ into (3) we obtain:

$$\begin{aligned}\rho\frac{\partial^2}{\partial t^2}(\nabla\Phi + \nabla\times\Psi) &= (\lambda+2\mu)\nabla(\nabla^2\Phi) -\\ &\quad \mu\nabla\times\nabla\times(\nabla\times\Psi)\end{aligned}$$

The right-hand side of the above equation comes from the fact that if we take the divergence of the displacement field, then:

$$\nabla\cdot\mathbf{u} = \nabla\cdot\nabla\Phi + \nabla\cdot(\nabla\times\Psi) = \nabla^2\Phi$$

Likewise, if we take the curl of the displacement field, then:

$$\begin{aligned}\nabla\times\mathbf{u} &= \nabla\times\nabla\Phi + \nabla\times\nabla\times\Psi\\ &= \nabla(\nabla\cdot\Psi) - \nabla^2\Psi\\ &= -\nabla^2\Psi\end{aligned}$$

noting the use of the vector identity:

$$\nabla^2\mathbf{v} = \nabla(\nabla\cdot\mathbf{v}) - \nabla\times\nabla\times\mathbf{v}$$

which is valid for any vector $\mathbf{v}$.

It is also assumed without loss of generality that $\nabla\cdot\Psi = 0$ — the vector potential has zero divergence. This can be done since taking the curl discards any part of the vector potential that would give rise to a non-zero divergence. Using the same vector identity as before, the second term on the RHS of the wave equation can be simplified as follows:

$$\begin{aligned}\nabla\times\nabla\times(\nabla\times\Psi) &= -\nabla^2(\nabla\times\Psi) + \nabla(\nabla\cdot(\nabla\times\Psi)) \\ &= -\nabla^2(\nabla\times\Psi)\end{aligned}$$

since the divergence of the curl is zero.

This now allows the wave equation to be re-organized as follows:

$$\nabla\left[(\lambda+2\mu)\nabla^2\Phi - \rho\frac{\partial^2\Phi}{\partial t^2}\right] = -\nabla\times\left[\mu\nabla^2\Psi - \rho\frac{\partial^2\Psi}{\partial t^2}\right] \tag{4}$$

One solution to the above equation can be obtained by setting both bracketed terms to zero. This yields two wave equations, one for each potential.

1. For P-waves (Compressional waves)

- The oscillatory variable $\mathbf{u} = \nabla\phi$ of P-waves or compressional waves is volumetric change, which is directly related to pressure.
- Setting the left bracket in (4) to zero, we obtain:

$$\frac{\partial^2\Phi}{\partial t^2} = \frac{\lambda+2\mu}{\rho}\nabla^2\Phi$$

  which clearly has the form of a scalar wave equation i.e.

$$\frac{\partial^2 f}{\partial t^2} = c^2\nabla^2 f$$

- The speed α at which this type of wave propagates is therefore given by:

$$\alpha = \sqrt{\frac{\lambda+2\mu}{\rho}}$$

2. For S-waves (Transverse waves)

- In contrast, the oscillatory variable $\mathbf{u} = \nabla\times\mathbf{\Psi}$ of S-waves implies a shear disturbance with no volume change ($\nabla\cdot\nabla\times\mathbf{\Psi} = 0$).
- Setting the right bracket in (4) to zero, we obtain:

$$\frac{\partial^2\Psi}{\partial t^2} = \frac{\mu}{\rho}\nabla^2\Psi$$

  which clearly has the form of a vector wave equation i.e.

$$\frac{\partial^2\mathbf{v}}{\partial t^2} = c^2\nabla^2\mathbf{v}$$

- The speed β at which this type of wave propagates is therefore given by:

$$\beta = \sqrt{\frac{\mu}{\rho}}$$

Final Result:

- **P-wave Equation:**
  $\rho\frac{\partial^2\phi}{\partial t^2} = (\lambda+2\mu)\nabla^2\phi$ with $v_P = \sqrt{\frac{\lambda+2\mu}{\rho}}$
- **S-wave Equation:**

$$\rho\frac{\partial^2\mathbf{A}}{\partial t^2} = \mu\nabla^2\mathbf{A} \quad \text{with } v_S = \sqrt{\frac{\mu}{\rho}}$$

2. Module 2: Identifying Shadow Zones

2.1. Explain what is meant by the "S-wave shadow zone" and why its existence indicates the presence of a liquid core.

Shearing S-waves are body waves that travel along the most direct routes within the Earth. Their behavior creates shadow zones that provide valuable insights into the Earth's structure. The S-wave shadow zone refers to an area on the Earth's surface where S-waves are not detected following an earthquake or other seismic event. The seismic shadows are the effect of seismic waves striking the core-mantle boundary

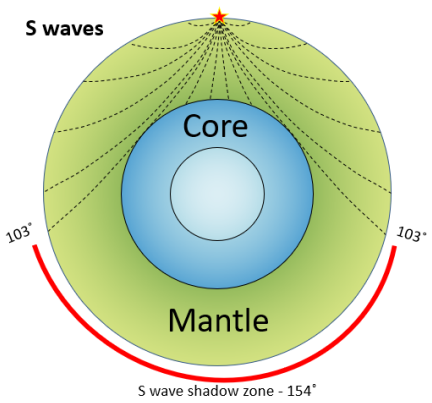

Figure 4: S-wave shadow zone of Earth.

In this illustration, an earthquake at the top of the globe produces shearing S-waves that radiate outward in all directions. As these waves encounter various boundaries at different depths, they refract and take on curved paths.

S-waves cannot travel through liquids because of the way they propagate. Unlike P-waves, which compress and expand materials as they move, S-waves move by shearing or shifting particles perpendicular to the direction of wave travel. This requires the medium to have shear strength, meaning it must resist shape changes.

Liquids, however, do not have shear strength—they flow and deform rather than resist shear forces. When an S-wave reaches a liquid, there is nothing to "push back" against the wave's motion, so it dissipates instead of propagating.

This is why at the core-mantle boundary, S-waves are completely stopped by the liquid outer core and seismologists observe an S-wave shadow zone on the opposite side of the Earth during earthquakes that extends beyond an angle of 104° for Earth.

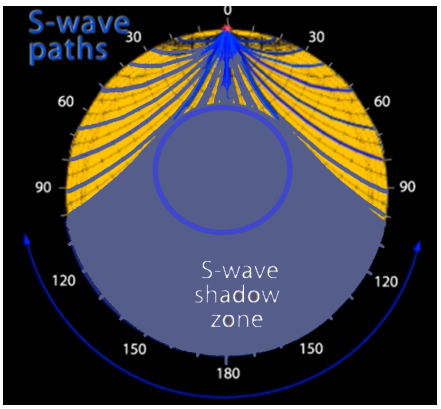

Figure 5: S-wave paths.

2.2. If S-waves are not detected on the opposite side of the planet from a seismic event, what can we infer about the core's state?

If S-waves are not detected on the opposite side of the Earth from the earthquake, it means the seismic waves passed through the Earth's interior and encountered a region (the outer core) that does not allow S-waves to pass.

The absence of S-waves in that region implies that the core cannot be solid in that area. This is evidence that the outer core might be a liquid, as a liquid layer would prevent S-waves from traveling through it.

3. Module 3: Calculating the Core-Mantle Boundary (CMB)

3.1. Use Snell's Law to explain how P-waves refract at the core-mantle boundary.

Consider a planar wavefront passing through a slow anomaly. Can this anomaly be detected by a seismic network located on the opposite side?
With increasing distance from the anomaly, the wavefronts undergo healing called Wavefront Healing.

According to ray theory:

$$T_A^B = \int_A^B \frac{dS}{C(s)},$$

Phase Conversions

Consider a descending P-wave that arrives at an interface, part of its energy is reflected, part of it is transmitted to the other side, and part of the reflected and transmitted energies are converted into $S_v - wave$.

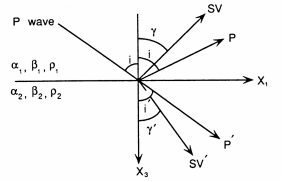

Figure 6

The angle of incidence of the reflected and transmitted waves is controlled by an extended form of Snell's law:

$$\frac{\sin i}{\alpha_1} = \frac{\sin \gamma}{\beta_1} = \frac{\sin i'}{\alpha_2} = \frac{\sin \gamma'}{\beta_2} \equiv P$$

Consider a plane wave propagating in the k direction. The apparent velocity c_1, measured at the surface is larger than the actual velocity, c.

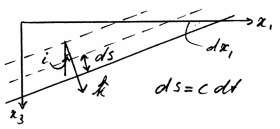

Figure 7

$$c_1 = \frac{c}{\sin i} > c$$

$$\sin i = \frac{ds}{dx_1} = \frac{cdt}{dx_1} = \frac{c}{c_1} \Rightarrow$$

$$P \equiv \frac{\sin i}{c} = \frac{1}{c_1}$$

Snell's Law for Radial Earth

The radial earth ray parameter is given by:

$$P \equiv \frac{R \sin i}{V}$$

Next, we present a geometrical proof showing that P is constant along the ray.

Geometrical Proof: A geometrical construction showing that $\frac{R \sin i}{V}$ is constant along the ray.

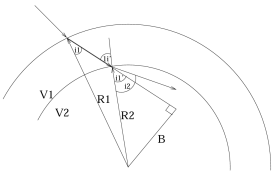

Figure 8

From the two triangles:

$$B = R_2 \sin i_1' = R_1 \sin i_1$$

From Snell's law across a plane boundary:

$$\frac{\sin i_1'}{\sin i_2} = \frac{V_1}{V_2} \tag{5}$$

$$\Longrightarrow \frac{R \sin i}{V} = \text{constant} = \text{ray parameter.}$$

Measurement of P

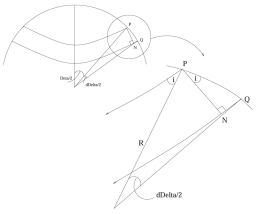

Figure 9

$$\sin i = \frac{QN}{QP} = \frac{V\,dT/2}{R\,d\Delta/2}$$

$$\implies \frac{dT}{d\Delta} = \frac{R\sin i}{V} = P$$

So, P is the slope of the travel-time curve (T-versus-Δ). While the units of the flat earth ray parameter are s/m, that of the radial earth is s/rad.

3.2. *Given the following data: v_1=10 km/s (mantle P-wave velocity), v_2=8 km/s (core P-wave velocity) and i=30°. Calculate the angle of refraction(r).*

Given $v_1 = 10km/s$, $v_2 = 8km/s$ here v_1 denotes mantle P-wave velocity and v_2 denotes core P-wave velocity, from the Figure 3 the angle of incidence i is denoted by i_1' and angle of refraction r is denoted by i_2 then our formula is as follow from equation (1)

$$\frac{sin\,i}{sin\,r} = \frac{v_2}{v_1}$$

Putting values we get :

$$\frac{sin\,30^\circ}{sin\,r} = \frac{8}{10}$$

$$sin\,r = \frac{10}{8} \times \frac{1}{2}$$

Solving we get

$$r = 38.6821^\circ$$

4. Module 4: Determining Core Radius

4.1. *The total radius of Mars is R=3390 km. The depth to the core-mantle boundary is d=560 km. Calculate the core radius (R_c) using the formula: $R_c = R - d$. Verify whether this calculated core radius is consistent with seismic data observations.*

We first calculate the core radius of Mars using the formula $R_c = R - d$ where

- R represents the total radius of Mars
- R_c represents the core radius of Mars
- d represents the depth of the core-mantle boundary

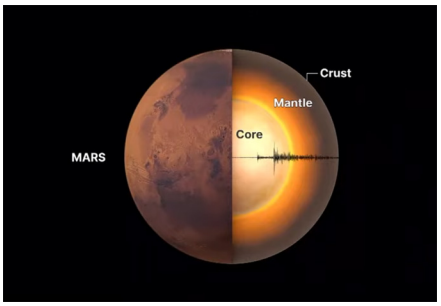

Figure 10: Structure of Mars

Using R=3390 km and d=560 km,

R_c=2830 km

This radius R_c is inconsistent with seismic data observations obtained from Module 7 which is 1830 km. The core radius of Mars is not verified since the given formula only removes the depth of the upper mantle from the total radius of Mars. If we also remove the depth of the lower mantle, we will get the correct answer.

5. Module 5: Verifying Core State

5.1. Introduction

Mars' interior has been a focal point for planetary scientists, especially with the seismic data provided by the InSight mission's Seismic Experiment for Interior Structure (SEIS). This study consolidates observations of S-wave absence and P-wave velocity reduction, alongside models of core formation, to analyze the state and composition of Mars' core. The findings have profound implications for understanding Mars' geodynamic evolution, magnetic field history, and broader planetary science.

5.2. Seismic Observations and Core Formation

Seismic observations have confirmed a liquid Martian core. Key indicators include the absence of S-waves, as shear waves cannot propagate through liquids, and reduced P-wave velocities, which correlate with sulfur-rich iron alloy compositions.

5.2.1. Key Observations

- Absence of S-waves in core regions indicates a liquid state.
- Reduction in P-wave velocities corresponds to sulfur-rich iron alloys.
- Inferred core density matches theoretical predictions for a sulfur-rich composition.
- Seismic shadow zones provide insights into core radius and physical properties.

5.3. Core Composition and Structure

5.3.1. Composition

The Martian core primarily comprises an iron-nickel alloy enriched with sulfur (estimated at 11–19 wt%). This composition lowers the melting point, favoring a liquid state under Martian core conditions. Additional light elements, such as oxygen, may also be present, influencing core density and phase behavior.

5.3.2. Dimensions and Stratification

Mars' core radius is estimated at 1600–1810 km. Stratification mechanisms include the formation of iron 'snow' and $Fe_{3-x}S_2$ 'ground fog,' creating compositional layers. Studies suggest a partially molten zone near the core-mantle boundary, contributing to thermal and chemical heterogeneities.

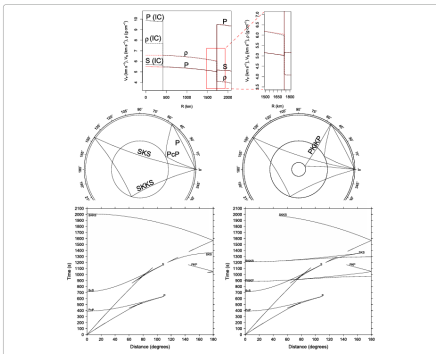

Figure 11: Schematic of core formation, showing material equilibration during accretion (CODE 1).

5.4. Seismic Velocity Profiles and Thermal Dynamics

5.4.1. Seismic Wave Behavior

The absence of S-waves within specific epicentral distances (40°–59°) and reduced P-wave velocities near the core boundary highlight the core's liquid state. Models indicate significant attenuation of seismic energy in the core region due to its fluid nature.

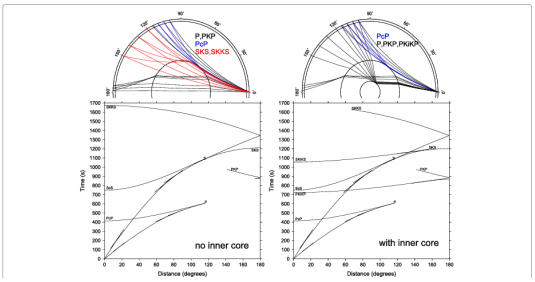

Figure 12: Comparison of compressional (P-wave) and shear (S-wave) velocity profiles in the Martian interior (CODE 1).

5.4.2. *Thermal Gradients and LVZ*

Thermal gradients ranging from 1.6–2.5 K/km and a mantle potential temperature of 1600–1700 K influence the low-velocity zone (LVZ) in the upper mantle. These gradients drive mantle convection and influence core cooling rates.

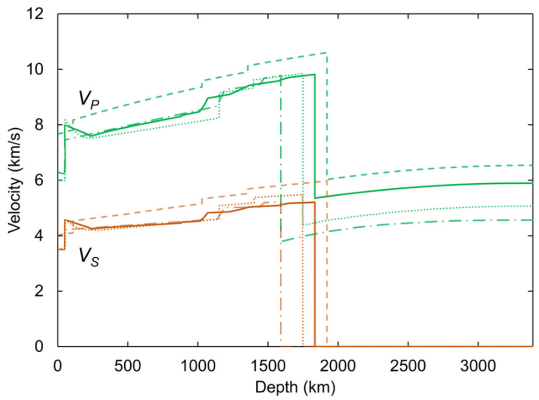

Figure 13: Seismic amplitude behavior with distance, showing the observed drop in S/P amplitude ratios within the LVZ (CODE 2).

5.5. *Magnetic Field and Implications for Planetary Evolution*

5.5.1. *Cessation of Magnetic Field*

Core stratification has inhibited vigorous convection, leading to the cessation of Mars' magnetic field. Estimated core-mantle boundary temperatures range from 1375–1575 K. Thermal conductivity and heat flow estimates suggest limited dynamo activity, consistent with magnetic anomalies observed in the crust.

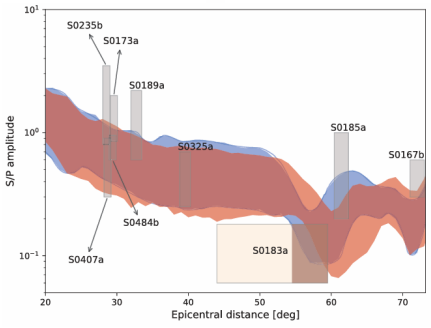

Figure 14: Relationship between core stratification and the cessation of Mars' magnetic field (CODE 3).

5.5.2. *Implications for Mars' Evolution*

The lack of a global magnetic field has exposed Mars' surface to solar wind, resulting in atmospheric erosion over billions of years. Understanding core dynamics provides insights into planetary habitability and long-term evolution.

5.6. *Future Research Directions*

5.6.1. *Detecting Inner Core Structures*

Advancements in seismic techniques may help identify potential inner core structures. Identifying a solid inner core would provide new constraints on the thermal and compositional state of Mars' interior.

5.6.2. *Refining Models of Core Formation*

High-pressure experiments and advanced simulations can refine models of core formation and evolution. These studies will improve predictions of planetary differentiation and chemical equilibration processes.

5.6.3. *InSight Mission Extensions*

Prolonging the InSight mission or deploying additional landers could enhance data quality and spatial coverage, enabling more accurate interior models.

5.6.4. Conclusion

Seismic and theoretical analyses confirm the liquid state of Mars' sulfur-rich core. Observations from the InSight mission provide new constraints for understanding the thermal and compositional dynamics of terrestrial planets. Future research will focus on detecting potential inner core structures, refining models of planetary formation, and exploring implications for Mars' habitability and evolution.

References

1.https://geo.libretexts.org/Bookshelves/Geology/Physical_Geology_(Earle)/09%3A_Earths_Interior/9.01%3A_Understanding_Earth_Through_Seismology

2. Chapter 3, Fundamentals of Geophysics by William Lowrie.

3. Shearer, P. M. (2009). *Introduction to Seismology*. Cambridge University Press.

4. Lay, T., Wallace, T. C. (1995). *Modern Global Seismology*. Academic Press.

5. https://mars.nasa.gov/insight/